Original article

Cephalalgia
An International Journal of Headache

International Headache Society

Cephalalgia
2026, Vol. 46(4) 1–13

DOI: 10.1177/03331024261416494
journals.sagepub.com/home/cep

Sage

Sex-specific orchestration of morphometric similarity networks in children and adolescents with migraine

Laura Papetti[1], Alessia Guarnera[2,3], Daniela Longo[2], Antonio Napolitano[4], Giulia Baldassari[4], Greta Pirani[4], Giorgia Sforza[1], Gabriele Monte[1], Fabiana Ursitti[1], Francesco Dellepiane[2], Maria Vaccaro[4], Alessia Carboni[2], Maria Camilla Rossi-Espagnet[2,3], Giulia Moltoni[2,3], Carlo Gandolfo[2], and Massimiliano Valeriani[1,5,6]

Abstract

Background: Migraine accounts for most primary headaches in children and adolescents and is related to cortical and connectivity changes. However, the underlying mechanisms remain unclear. Morphometric similarity mapping has not yet been applied to children and adolescents with migraine.

Methods: Eighty-three patients (6–17 years) with migraine without aura and 81 age- and sex-matched controls were retrospectively included. High-resolution 3D T1-weighted and diffusion-weighted magnetic resonance imaging scans were processed to extract cortical morphometric parameters and compute morphometric similarity networks (MSN). Global and regional MSN differences were assessed between patients and controls, and across subgroups defined by sex, attack frequency and migraine-associated symptoms.

Results: Patients showed significant MSN alterations, particularly in temporal and cingulate regions. Sex emerged as the strongest factor influencing MSN architecture, with additional modulations linked to attack frequency and clinical symptoms. Affected pathways encompassed the executive control, nociceptive and default mode networks.

Conclusions: Migraine in children and adolescents is associated with widespread MSN abnormalities, likely reflecting cortical reorganization mechanisms. Male and female patients appear to engage distinct neural "orchestras", each emphasizing different network sections (sensory–affective in males and cognitive–attentive in females) to produce a shared clinical experience. These findings highlight sex as a key determinant of migraine neurobiology in developmental age.

Keywords

cortical abnormalities, cortical morphometry, headache, migraine, morphometric similarity, pediatric

Date received: 22 March 2024; accepted: 13 December 2025

Introduction

The World Health Organization identifies migraine as the most common neurological condition and one of the most disabling diseases worldwide, with a significant social and economic burden (1). Current evidence suggests that migraine is a complex and progressive disorder (2), arising from the interaction between individual predisposition and disease-driven neurological processes (2,3) and leading to structural and functional brain alterations (2–4). These abnormalities indicate the activation of cerebral plasticity (5), already documented in patients with long-standing headaches and in those treated with anti-migraine drugs (5–7).

[1]Developmental Neurology Unit, Bambino Gesù Children's Hospital, IRCCS, Rome, Italy
[2]Functional and Interventional Neuroradiology Unit, Bambino Gesù Children's Hospital, IRCCS, Rome, Italy
[3]Neuroradiology Unit, NESMOS Department, Sant' Andrea Hospital, La Sapienza University, Rome, Italy
[4]Medical Physics Unit, Bambino Gesù Children's Hospital, IRCCS, Rome, Italy
[5]Center for Sensory-Motor Interaction, Aalborg University, Aalborg, Denmark
[6]Systems Medicine Department, Tor Vergata University of Rome, Rome, Italy

Laura Papetti, Alessia Guarnera, Daniela Longo and Massimiliano Valeriani contributed equally to this study.

Corresponding author:
Antonio Napolitano, Medical Physics Department, Bambino Gesù Children's Hospital IRCCS, 00165 Rome, Italy.
Email: antonio.napolitano@opbg.net

Recent literature has proposed a pathophysiological model in which migraine disrupts and reshapes brain connectome topography (8), supporting the concept of migraine as a "connectopathy" (9). Nonetheless, findings remain heterogeneous, and no specific "morphological signature" of migraine has yet been defined (10–12).

Morphometric similarity mapping (MSM) is a novel technique for studying cortical organization and brain connectivity (13). It quantifies morphometric similarity among cortical regions by integrating multiple magnetic resonance imaging (MRI)-derived parameters to reconstruct a whole-brain anatomical–functional network (13,14). Regions showing higher similarity are assumed to be more likely axonally connected (15), allowing MSM to provide an indirect measure of the connectome. Importantly, MSM requires only standard MRI acquisitions (16) and has already proven effective in conditions such as schizophrenia (13,14) and Alzheimer's disease (17), as well as in studies of cognitive performance (14,17). Only a few studies have applied MSM to adult migraine cohorts (18,19), while, to our knowledge, it has never been used in children and adolescents with migraine without aura (MwoA).

The aims of the present study were threefold: (i) to identify differences in morphometric similarity (MS) between children and adolescents with MwoA and healthy controls; (ii) to explore morphometric similarity networks (MSN) alterations within patient subgroups defined by demographic and clinical characteristics; and (iii) to examine potential correlations between MSN measures and these variables.

Methods

Design and participants

Patients were retrospectively identified by reviewing the Bambino Gesù Hospital imaging archive between January 2018 and July 2023 using the keywords "migraine", "headache" and "cephalalgia". Two neuroradiologists (with 32 years and eight years of experience, respectively) independently reviewed 498 MRIs; discrepancies were resolved by consensus.

Subjects with high-quality MRI scans including diffusion-weighted imaging (DWI) and 3D T1 magnetization prepared rapid gradient echo (MPRAGE) sequences, and without signal or morphological abnormalities, were considered eligible. Once subjects with suitable MRI data were identified, two neurologists reviewed their medical records to assess the presence of exclusion criteria, which included abnormal neurological examination; migraine with aura; other primary headache disorders; sleep, neurological, neuropsychiatric or systemic disorders; maternal diseases during pregnancy; recent use of migraine prophylactic treatments; or MRI performed during an acute attack. After identifying potential participants with headache, they were interviewed to confirm that, at the time of the MRI examination, they fulfilled the International Classification of Headache Disorders, 3rd edition (ICHD-3) criteria (20) for MwoA. The final enrolled subjects were divided into subgroups according to the following characteristics at the time of MRI: sex; monthly migraine days (MMD); presence or absence of nausea/vomiting; and presence or absence of photophobia/phonophobia. Regarding MMD, patients were classified as having low-frequency migraine (<5 MMD) or high-frequency migraine (≥5 MMD). This cut-off was chosen for two main reasons: first, 5 MMD is generally considered the threshold for initiating prophylactic treatment in children and adolescents with migraine (21) and, second, unlike in adult migraine (22), there is no consensus in pediatric populations on other parameters to distinguish different severity phenotypes within episodic migraine.

The control group included subjects with high-quality MRI scans without abnormalities. They were interviewed and neurologically assessed to exclude underlying disorders and migraine. The selection process of the study population is summarized in the flow diagram (Figure 1). Notably, 68 patients and 74 controls had been included in a previous study by Guarnera et al. (23).

The study was conducted in accordance with the Declaration of Helsinki and approved by the Institutional Research Committee. Informed consent was obtained from all patients or their parents before MRI examination.

MRI protocol

Patients and controls underwent high-quality brain MRIs on the same 3T scanner (Magnetom Skyra; Siemens, Erlangen, Germany) with a 32-channel brain coil (length × width × height: 440 × 330 × 370 mm) and the following protocol: axial DWI (repetition time (TR) 6400 ms, echo time (TE) 98 ms, flip angle (FA) 75°, slice thickness (ST) 4 mm); sagittal 3D T1 MPRAGE (TR 1570 ms, TE 2.67 ms, inversion time (TI) 900 ms, FA 9°, ST 0.8 mm); axial turbo spin-echo T2 (TR 6380 ms, TE 109 ms, ST 3 mm); coronal turbo spin-echo T2 (TR 6380 ms, TE 109 ms, FA 150°, ST 3 mm); axial fluid-attenuation inversion recovery (TR 9000 ms, TE 81 ms, TI 2500 ms, FA 150°, ST 3 mm).

Data processing

For each subject, we estimated eleven morphometric features divided into three classes and derived from two MRI sequences: 3D T1 MPRAGE and DWI. The morphometric features identified for the MSN (13) are illustrated in the supplementary material (Figure S1). Standard sequences such as 3D T1 MPRAGE and DWI were chosen over advanced sequences with longer acquisition times that may reduce image quality (24). 3D T1 MPRAGE data were preprocessed with FreeSurfer v7 (http://surfer.nmr.mgh.harvard.edu) using a standard automatic pipeline (i.e. recon-all) (25) that sequentially performed skull stripping, removal of non-brain tissue,

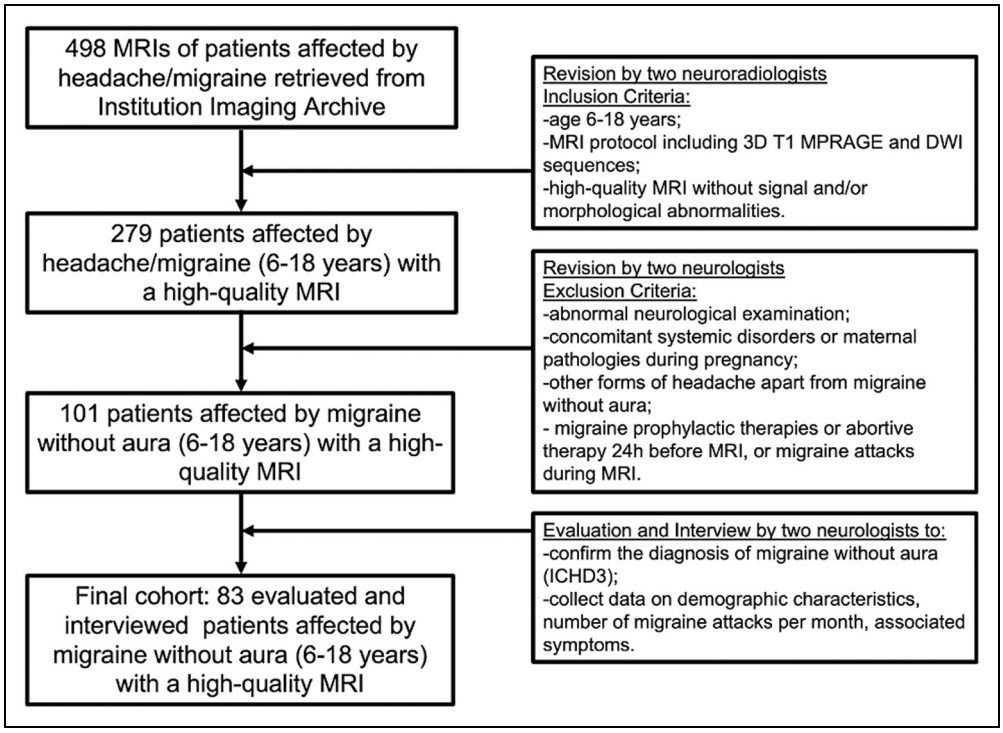

Figure 1. Flow chart of patients. The flow diagram describes patients' selection highlighting the inclusion and exclusion criteria that resulted in the final cohort. DWI = diffusion weighted imaging; ICHD-3 = International Classification of Headache Disorders, 3rd edition; MPRAGE = magnetization prepared rapid gradient echo; MRI = magnetic resonance imaging;

motion correction and transformation to Talairach-Tournoux space, to generate grey matter (GM) and white matter (WM) segmentation. The inner cortical surface (white surface) was generated using the Freesurfer pipeline by tessellating the GM–WM boundary. In contrast, the outer surface (pial surface) was generated by expanding the white surface with point-to-point matching. The cortical thickness (CT), surface area (SA), GM, curvature index (CI), folding index (FI), mean curvature (MC), Gaussian curvature (GC) parameters were calculated by the Freesurfer automatic recon-all pipeline. CT was measured as the average shorter distance measured between the estimated grey/white and pial surfaces according to the Fischl and Dale approach (26). SA was computed as the total of the areas of all vertices falling within a region (27). The regional GM volume was the sum of the voxels in a region. The parameter CI represents the maximum intrinsic curvature across all points within the surface (28). FI was calculated as the number of cortices buried within the sulcal folds compared to the number of cortices on the visible outer cortex (29). MC was calculated as the reciprocal of the radius of the inscribed circle for each vertex, and the signs of the gyrus and sulcus were opposite (30). The GC curvature of a surface at a given point was the product of the principal curvatures, which were the eigenvalues of the shape operator at the point (31). Sulcal depth (SD) and gyrification height (GH) were obtained from sulcal surface maps generated by Freesurfer. SD measured the distance a given vertex moves outward during the inflation process while GH was considered as the distance above the average surface at each vertex. The local gyrification index (LGI) is computed at the vertex level over the entire cortex using the adaptive kernel approach which incorporates gyral crowns and the neighbouring sulcal fundi proposed by Lyu et al. (32). Diffusion data were processed with the correction of the gradient non-linearity, eddy current and echo-planar imaging distortion (33). From DWI acquisition, the mean diffusivity (MD) value was calculated as the average diffusion motion of water molecules independent of directionality and then projected onto the pial brain surface via Freesurfer.

MSN analysis

MSN analysis was performed for each participant using the 68 cortical regions defined by the Desikan–Killiany atlas (34). For every subject, we computed a single individual MS matrix (68×68), representing the pattern of inter-regional morphological similarity across the cortex. Each cortical region was characterized by eleven morphometric features derived from T1-weighted and diffusion MRI data (CT, SA, GM, CI, FI, MC, GC, SD, GH, LGI and MD).

Table 1. Demographic and clinical characteristics of patients and controls.

	Patients with MwoA			Controls		
Characteristic	Females, n (%) 46 (55.4)	Males, n (%) 37 (44.6)	Total (n = 83)	Females, n (%) 40 (49.3)	Males, n (%) 41 (50.7)	Total (n = 81)
Age (years), mean ± SD	11.75 ± 3.36	11.25 ± 2.83	11.5 ± 3.12	11.44 ± 3.35	11.71 ± 3.18	11.1 ± 3.45
MMD, n (%)						
<5	24 (52.2)	19 (51)	43 (51.8)	–	–	–
≥5	22 (47.8)	18 (49)	40 (48.2)	–	–	–
Symptoms, n (%)						
Photophobia/phonophobia present	40 (87)	31 (83.7)	71 (85.5)	–	–	–
Photophobia/phonophobia absent	6 (13)	6 (16.3)	12 (14.5)	–	–	–
Nausea/vomiting present	26 (56.5)	19 (51.3)	45 (54.2)	–	–	–
Nausea/vomiting absent	20 (43.5)	18 (48.7)	38 (45.8)	–	–	–

MMD = monthly migraine days; MwoA = migraine without aura.

Each morphometric feature vector was normalized using *Z*-scores across regions to account for variations in value distributions across features. Pearson's correlation coefficients were then calculated between the morphometric feature vectors of each pair of cortical regions. Each cell of the MS matrix therefore represents the correlation between two regions based on their multifeatured morphometric profile. This procedure resulted in the subject-specific MS matrix (M*i*), where each cell represents the correlation between two cortical regions based on their multifeatured morphometric profiles.

The global mean MS and the regional mean MS were calculated. The global mean morphometric similarity for each participant is the average of all correlations in M*i*. For each individual, we also estimated the MS of each region to the rest of the regions in the brain by averaging the edge weights connecting it to all other nodes. In particular, the regional mean MSN_{iJ} for the i_{th} participant at each region $j = 1$–68 is the average of the jth row (or column) of M*i*. Thus, regional MS strength is equivalent to the weighted degree or hubness of each regional node, connected to all other nodes in the whole brain connectome represented by the morphometric similarity matrix (14).

Statistical analysis

Statistical analyses were performed using the MATLAB Statistics and Machine Learning Toolbox (version 2017a) (MathWorks Inc., Natick, MA, USA). Two linear models were implemented. Model 1 examined differences in MS between patients with MwoA and healthy controls, including age, sex and group (MwoA or control subjects) as predictors, together with the interaction between group and sex and the interaction between group and age. Model 2 assessed associations between MS and clinical features within the migraine group only, using age, sex, monthly migraine days (MMD), nausea/vomiting and photophobia/phonophobia as predictors, as well as their interactions with sex. Both models were applied to global MS and to regional MS values (68 cortical regions). Full model specifications and model equations are reported in the methods section of supplementary materials.

For each fitted linear model, the significance of individual predictors and interaction terms was evaluated using the analysis of variance (ANOVA) table of the linear model (*F*-tests), as provided by the anova(mdl) function in MATLAB. This procedure corresponds to standard tests of fixed effects within a general linear modeling framework. Significant effects were further explored using post-hoc linear analyses to determine the direction of the associations.

Multiple comparisons across cortical regions were corrected using the false discovery rate (FDR) ($q < 0.05$). All *p*-values reported in the main text and the TableS1-S4 to FDR-corrected values (*p*-FDR). A detailed description of the statistical models, analytical workflow and the full ANOVA is provided in the methods section of supplementary materials.

Results

Participants

In total, 279 patients aged 6–18 years with high-quality MRI scans, including DWI and 3D T1 MPRAGE sequences and without signal or morphological abnormalities, were initially considered eligible. Among these, 101 patients fulfilled the ICHD-3 criteria for MwoA. After applying exclusion criteria, the final cohort consisted of 83 patients with MwoA (46 females), all with normal MRI findings (Figure 1).

The control group comprised 81 healthy subjects (41 females; aged 6–18 years) with normal, high-quality MRI scans. The main demographic and clinical characteristics of patients with migraine and control subjects are summarized in Table 1. The mean ± SD age of patients with MwoA was 11.5 ± 3.12 years, while that of control subjects was 11.1 ± 3.45 years ($p > 0.05$).

Morphometric similarity networks

The full data from the ANOVA tables of the linear models used as a preliminary filtering step are reported in the supplementary material (Tables S1–S4). As expected for MS analyses, the models showed small effect sizes and modest explained variance, which is consistent with previous literature in structural neuroimaging (13,35).

In the following sections, we present the results of the final post-hoc linear analyses, which clarify the specific associations underlying the observed effects. Age did not show any significant effect on MS values in any of the analyses.

Patients vs. controls

At the global level, the anova table of the fitted linear model indicated that group (patients vs. controls) was the only predictor showing a significant effect ($F = 4.81$, $p = 0.03$, explaining a modest portion of the variance ($R^2 = 0.11$, adjusted $R^2 = 0.07$, $\eta^2 = 0.038$). Neither age, sex, nor their interactions reached statistical significance, with corresponding η^2 values close to zero (<0.001–0.001).

At the regional level, post-hoc analyses revealed significant group effects and sex × group interactions across specific cortical areas, with small effect sizes ($\eta^2 \approx 0.028$–0.047). The corresponding regional model fits were modest ($R \approx 0.26$–0.32; $R^2 \approx 0.07$–0.10). Full statistical details are reported in the methods section of supplementary materials.

Post-hoc analysis revealed that patients with MwoA showed significantly increased MS in the left superior temporal sulcus ($p < 0.02$) (Figure 2A), left middle temporal gyrus ($p < 0.005$) (Figure 2A), left inferior temporal gyrus ($p < 0.01$) (Figure 2A) and left caudal anterior cingulate ($p < 0.02$) (Figure 2C), while decreased MS was observed in the right frontal pole ($p < 0.05$) (Figure 2B, D) compared to controls.

When stratified by sex, male patients exhibited increased MS in the left superior temporal sulcus ($p < 0.001$) (Figure 2E) and left caudal anterior cingulate gyrus ($p < 0.002$) (Figure 2G) and decreased MS in the left cuneus ($p < 0.01$) (Figure 2F, H) compared to male controls. Female patients showed increased MS in the left rostral anterior cingulate gyrus ($p < 0.03$) (Figure 2I) compared to female controls.

Patient subgroups

Regarding Model 2, the global MS analysis indicated that only the sex × MMD ($F = 4.87$, $\eta^2 = 0.041$; $p < 0.05$) and sex × vomiting/nausea ($F = 7.20$, η^2 0.046; $p < 0.01$) interactions reached statistical significance. The overall model accounted for a modest proportion of variance ($R^2 = 0.14$, adjusted $R^2 = 0.09$). All main effects (age, sex, MMD, vomiting/nausea, photophobia/phonophobia) and the remaining interaction terms (age × sex, sex × photophobia/phonophobia) were non-significant ($p > 0.05$), with corresponding effect sizes in the negligible range ($\eta^2 < 0.001$–0.007). At the

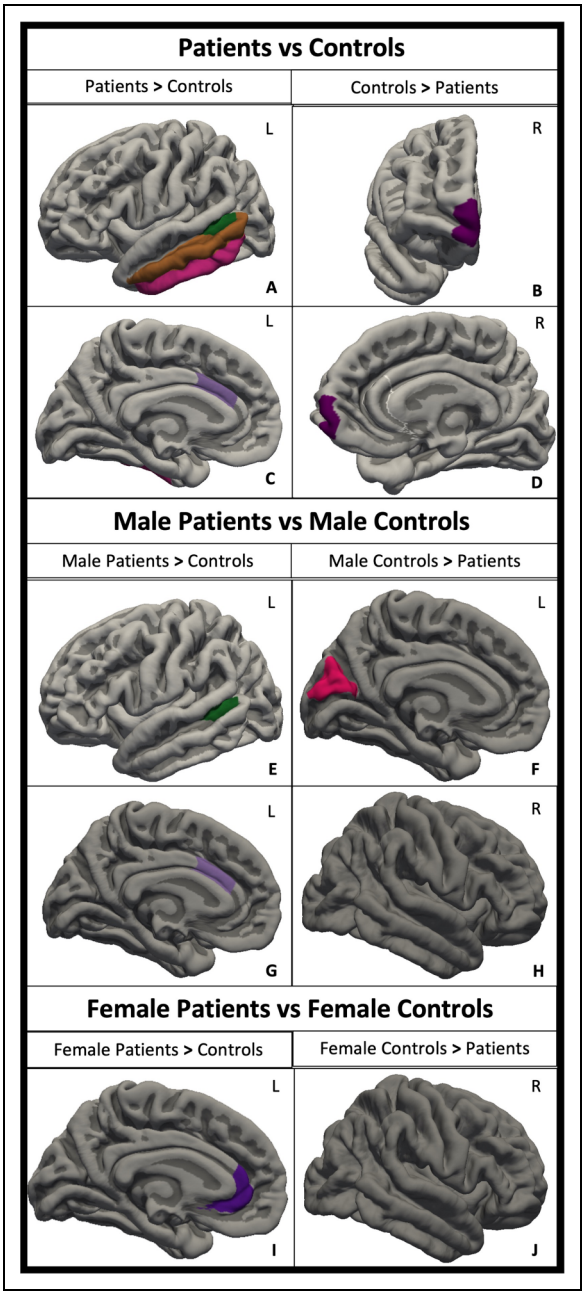

Figure 2. Results of the morphometric similarity networks analysis comparing patients with migraine without aura (MwoA) and controls. Brain regions showing significant differences in morphometric similarity values between patients with MwoA and controls (A–D), male patients and male controls (E–H) and female patients and female controls (I, J). L = left; R = right, > = increased; < = decreased. Colors highlight the cortical areas where significant effects were observed. Dark green: superior temporal sulcus (A, E); orange: middle temporal gyrus (A); magenta: inferior temporal gyrus (A); purple: frontal pole (B, D); light violet: caudal anterior cingulate gyrus (C, L); red: cuneus (F); dark violet: rostral anterior cingulate gyrus (I).

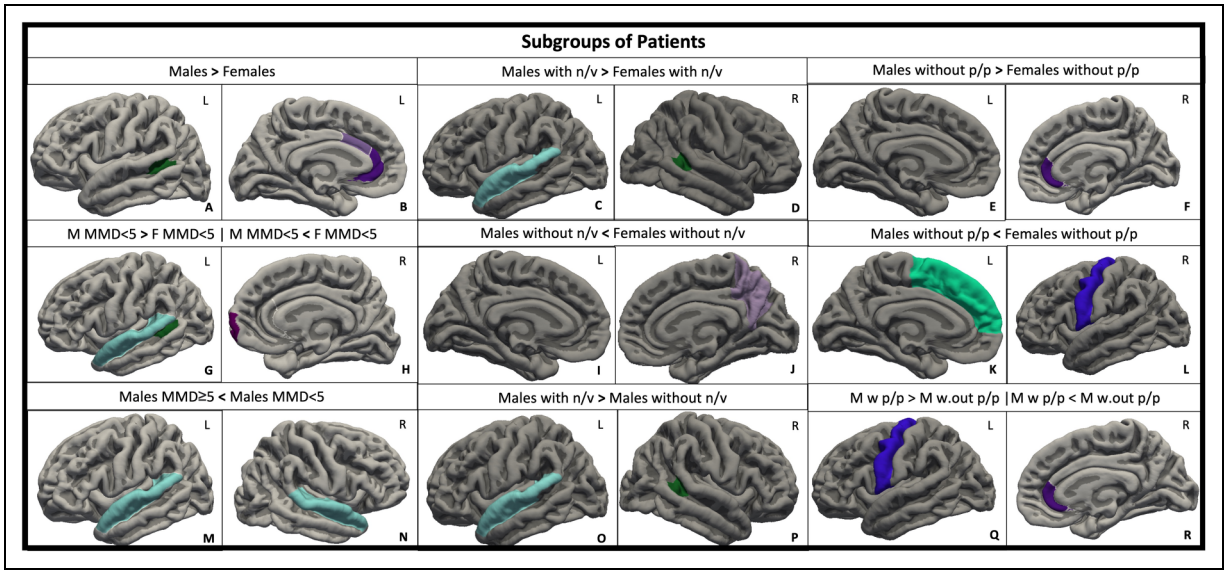

Figure 3. Results of the morphometric similarity networks analysis performed within subgroups of patients. Brain region showing significant differences in morphometric similarity values between patients subgroups: males and females (A,B); male with monthly migraine days (MMD) < 5 and female with MMD < 5 (G,H); males with MMD ≥ 5 and males with MMD < 5 (M,N); males with n/v and females with nausea and or vomiting (n/v) (C,D); males without n/v and females without n/v (I,J); males with n/v and males without n/v (O,P); males without photophobia and/or phonophobia (p/p) and females without p/p (E,F,K,L); males with p/p and male without p/p (Q, R). MS: morphometric similarities; L = left; R = right; w = with; w.out = without; F = females; M = males. Colors highlight the cortical areas where significant effects were observed. Dark green: superior temporal sulcus (A, D, P); dark violet: rostral anterior cingulate gyrus (B, F, R); light violet: caudal anterior cingulate gyrus (B); cyan: superior temporal gyrus (C, G, M, N, O); purple: frontal pole (H); pink: precuneus (J); green: superior frontal gyrus (K); blue: precentral gyrus (L, Q).

regional level, Model 2 revealed significant sex MMD and sex × vomiting/nausea interactions across multiple cortical areas. Effect sizes were small ($\eta^2 \approx 0.018$–0.062), with F-values ranging from 3.84 to 7.88. These effects correspond to plausible regional model fits in the range of $R \approx 0.20$–0.35 ($R^2 \approx 0.04$–0.12). Full regional results of exploratory analysis are reported in the supplementary material.

Post hoc analysis showed that in the subgroup comparisons, male patients showed increased MS in the left superior temporal sulcus ($p < 0.005$) (Figure 3A), left caudal anterior cingulate ($p < 0.02$) (Figure 3B) and rostral anterior cingulate gyrus ($p < 0.005$) (Figure 3B) compared to female patients. Moreover, males with MMD < 5 displayed increased MS in the left superior temporal sulcus and gyrus ($p < 0.001$) (Figure 3G) and decreased MS in the right frontal pole ($p < 0.001$) (Figure 3H) compared to females with MMD < 5. Within the male group, patients with MMD < 5 also showed increased MS in the bilateral superior temporal gyri compared to those with MMD > 5 ($p < 0.001$) (Figure 3M, N).

With respect to migraine-associated symptoms, males with nausea/vomiting exhibited increased MS in the left superior temporal gyrus ($p < 0.001$) (Figure 3C) and right superior temporal sulcus ($p < 0.001$) (Figure 3D) compared to females with the same symptoms, while males without nausea/vomiting showed decreased MS in the right precuneus ($p < 0.001$) (Figure 3J) compared to females without these symptoms. Within males, those with nausea/vomiting displayed increased MS in the left superior temporal gyrus ($p < 0.001$) (Figure 3O) and right superior temporal sulcus ($p < 0.001$) (Figure 3P) compared to those without symptoms.

Finally, in male patients with photophobia/phonophobia, we observed increased MS in the left precentral gyrus ($p < 0.005$) (Figure 3Q) and decreased MS in the right rostral anterior cingulate gyrus ($p < 0.001$) (Figure 3R) compared to males without these symptoms. Males without photophobia/phonophobia showed decreased MS in the left superior frontal gyrus ($p < 0.001$) (Figure 3K) and left precentral gyrus ($p < 0.002$) (Figure 3L) and increased MS in the right rostral anterior cingulate gyrus ($p < 0.001$) (Figure 3E, F) compared to females without symptoms.

Discussion

The analysis of MSN identified cortical pattern differences between children and adolescents affected by migraine without aura compared to controls and among the subgroups of patients (Table 2). Notably, differences in MSN were mostly related to sex and partly related to patients' clinical features such as the number of migraine attacks per month, the presence of nausea and/or vomiting, and the concomitant photophobia and/or phonophobia.

Table 2. Results from regional morphometric similarity networks analysis.

	Left hemisphere – gyri									Right hemisphere – gyri				
Comparisons	Superior frontal	Precentral	Superior temporal	Superior temporal sulcus	Middle temporal	Inferior temporal	Caudal anterior cingulate	Rostral anterior cingulate	Cuneus	Frontal pole	Superior temporal	Superior temporal sulcus	Rostral anterior cingulate	Precuneus
Patients vs. controls (direction and *p*-value)														
Total patients vs. Total controls				Higher < 0.02	Higher < 0.005	Higher < 0.01	Higher < 0.02			Lower < 0.05				
M patients vs. M controls				Higher < 0.001			Higher < 0.002		Lower < 0.01					
F patients vs. F controls								Higher < 0.03						
Subgroups (direction and *p*-value)														
M patients vs. F patients				Higher < 0.005			Higher < 0.02	Higher < 0.005						
M patients MMD < 5 vs. F patients MMD < 5			Higher < 0.001	Higher < 0.001						Lower < 0.001				
M patients MMD < 5 vs. M patients MMD ≥ 5			Higher < 0.001								Higher < 0.001			
M patients – n/v vs. > F patients – n/v			Higher < 0.001									Higher < 0.001		
M patients – n/v vs. M patients – without n/v			Higher < 0.001									Higher < 0.001		
M patients – without n/v vs. F patients – without n/v														Lower < 0.001
M patients with p/p vs. M patients – without p/p		Higher < 0.005											Lower < 0.001	
M patients – without p/p vs. F patients – without p/p	Lower < 0.001	Lower < 0.002											Higher < 0.01	

F = females; M = males; MMD = number of migraine attacks per month; n/v = nausea and/or vomiting; p/p = photophobia and/or phonophobia. All *p*-values are false discovery rate corrected.

The role of sex

Recent evidence highlights that migraine in both adults and youths is characterized by pronounced sex-related differences in prevalence, clinical features and treatment response, paralleled by structural and functional brain disparities (23,36–39). Our findings align with this view, showing that sex exerts a strong modulatory influence on MSN organization during developmental age (36).

When stratified by sex, male and female patients exhibited distinct patterns of MSN alterations. Males showed greater MS predominantly in temporal and cingulate regions, whereas females displayed higher MS in frontal and parietal areas. Additional sex-linked variations emerged in relation to attack frequency and migraine-associated symptoms such as photophobia, phonophobia and nausea/vomiting.

The distinct distribution of MSN abnormalities likely reflects the interplay between hormonal modulation, developmental trajectories and network-specific cortical organization (38–41). Previous morphometric studies have reported cortical thickening in the supplementary motor area, precuneus, basal ganglia and amygdala in female pediatric patients compared to males and controls (7,37,42), whereas temporal lobe alterations have been more frequently described in males (23). Moreover, Li et al. (18) demonstrated decreased MS in the superior temporal gyri and increased MS in the pars triangularis of women with menstrual related migraine.

Together, these data indicate that sex differences in MSN topology involve distinct large-scale networks. In males, the predominance of alterations in temporal and cingulate regions, comprising areas implicated in multisensory integration, auditory and visual processing, affective regulation, and pain modulation (43–45), suggests enhanced engagement of sensory and affective pathways. In contrast, females showed increased MS in frontal regions and the right precuneus, which are critically involved in cognitive control, top-down modulation, attentional processes, and self-referential functions (46–48).

These findings suggest that, although male patients may rely more heavily on sensory and affective networks, female patients may engage cognitive and attentive networks. Male and female brains appear to orchestrate migraine-related network activity in different ways, analgous to distinct orchestras performing the same symphony, each emphasizing unique sections to convey a shared clinical experience.

Frontal regions

In our cohort, sex-related differences within the frontal lobe were mainly observed in the frontal pole, superior frontal and precentral gyri. Male patients with low attack frequency (MMD < 5) showed decreased MS in the right frontal pole compared to females, while males without photophobia or phonophobia displayed reduced MS in the superior frontal and precentral gyri relative to females. Conversely, males with photophobia or phonophobia exhibited increased MS in the precentral gyrus compared to males without these symptoms.

Functionally, the frontal pole is a critical hub of the executive control network, involved in high-order executive processes (49–51), self-regulation, planning, and top-down modulation of emotional and pain responses (52–57). Reduced MS in this region in males with few attacks compared to females may suggest that, even at low levels of clinical burden, boys show less efficient engagement of prefrontal regulatory networks. This could represent an early vulnerability in cognitive control circuits, which may not yet translate into higher attack frequency but could act as a marker of predisposition.

The precentral gyrus, traditionally considered part of the nociceptive network, cooperates with postcentral and supramarginal cortices to encode the intensity, spatial location and sensory-discriminative aspects of pain (54–57). Alterations in these areas, particularly in relation to photophobia and phonophobia, are consistent with the idea that migraine symptoms are linked to disrupted integration between motor-executive and sensory processing networks (49).

Taken together, these results support previous morphometric studies on migraine in adults (51,52,58,59) and children (10,23,60–62), which have consistently reported reduced cortical thickness in frontal regions and impaired executive control network functioning in migraine patients. Differences in MS between female and male patients in relation to phonophobia are consistent with previous studies on the gyrification of the auditory cortex, which may help explain the higher incidence of phonophobia observed in male patients (23,38,63). Our data extend this evidence by showing that MSN alterations in the frontal lobe are not uniform but are modulated by sex and specific symptoms, pointing to distinct neurobiological pathways underlying similar clinical presentations.

Temporal regions

In our cohort, temporal regions showed some of the most consistent alterations. Patients exhibited increased MS in the left superior, middle and inferior temporal gyri and in the superior temporal sulcus compared to controls. These changes were mainly driven by male patients, who showed higher MS in superior temporal areas, particularly those with lower attack frequency or with nausea and vomiting, highlighting the contribution of temporal cortices to sex- and symptom-related effects.

Functionally, the superior temporal gyrus and sulcus are implicated in auditory and visual integration, language and social-emotional processing (64–66), and also play a role in the short-term memory of painful experiences (67). In the context of migraine, these regions have been linked to the mismatch between pain expectation and perception, as

well as to the attribution of emotional salience to painful experiences (68). Alterations in these regions may reflect abnormal coupling between sensory and affective components of pain processing, comprising a mechanism that could underlie the heightened sensory reactivity and emotional distress characteristic of migraine attacks (69).

Through their strong connections with limbic and insular cortices, temporal regions may also contribute to the autonomic and interoceptive components of migraine (70). Altered MSN in these areas could reflect abnormal integration of sensory and visceral signals, potentially explaining the occurrence of nausea and vomiting during migraine attacks (71).

Previous morphometric studies have reported reduced cortical thickness in the superior and middle temporal gyri of migraine patients (66,72,73), while functional MRI studies showed impaired connectivity of the middle temporal gyrus with cortical and subcortical pain-processing regions (5). Li et al. (18) further emphasized the involvement of the temporal lobes in migraine, showing that female patients with menstrual related migraine exhibited decreased MS in the right and left superior temporal gyri. Taken together with our findings, this evidence suggests that temporal regions may differentially mediate pain perception and expression according to sex. Since these alterations were observed in patients with low attack frequency, they do not appear to reflect the cumulative burden of the disease but rather early changes that may represent a marker of neurobiological vulnerability to migraine.

Anterior cingulate cortex

In the present study, patients with migraine showed increased MS in the left caudal anterior cingulate compared to controls, while sex-stratified analyses revealed further alterations: males exhibited increased MS in the caudal anterior cingulate and females in the rostral anterior cingulate. Functionally, the anterior cingulate cortex (ACC) is a key component of the limbic system and executive control network (74–76), with roles in emotional processing, pain modulation, conflict detection and decision-making (75–78). By linking emotional outcomes to behavior, the ACC contributes to both the affective dimension of pain and the regulation of cognitive control (79,80). Together with the anterior insula, it forms the salience network, which assigns relevance to sensory inputs and directs attentional resources (78).

Neuroimaging evidence consistently points to the ACC as a central node in migraine pathophysiology (49,80). Reduced activation and volume have been observed in patients with high-frequency migraine (80), whereas other studies have demonstrated increased functional connectivity between the ACC and frontal or temporal cortices (59,81,82). These alterations are consideredto reflect both disruption and compensatory recruitment of nociceptive and executive networks. In pediatric cohorts, atrophy of the cingulum together with frontal and temporal changes has been proposed as a phenotypic biomarker of migraine (61). Disrupted MSN architecture in this region may therefore underlie both the heightened emotional reactivity and the attentional disturbances commonly reported in migraine (69), with sex-specific alterations suggesting that males and females may engage this interface in distinct ways.

Cuneus

In our cohort, male patients exhibited decreased MS in the left cuneus compared to male controls. Traditionally, the cuneus has been associated with visual processing modulated by attention, working memory and reward expectation (83,84). More recent evidence has extended its role to higher-order functions, including cognitive processing, multisensory integration and the retrieval of emotionally salient perceptual experiences (85). Disrupted connectivity in the cuneus may contribute to abnormal sensory integration and misperception, as well as altered cognitive appraisal of external stimuli.

Previous morphometric studies have shown reduced cortical thickness in the cuneus of patients with migraine without aura (86), comprising findings that align with the MSN alterations observed the present study. Moreover, cuneus involvement has also been documented in other chronic pain conditions (87), reinforcing the idea that persistent craniofacial pain reshapes posterior cortical regions. The fact that, in our sample, MSN alterations of the cuneus were only identified in male patients raises the hypothesis that sex-specific biological factors, such as hormonal influences, may contribute to the vulnerability of posterior visual and multisensory networks in migraine.

Precuneus

In our cohort, sex-related effects were observed in the precuneus, where males without nausea or vomiting showed decreased MS compared to females. The precuneus lies in the medial parietal cortex and is a core hub of the default mode network (DMN), which is engaged during self-referential thought and internal mentation and has been shown to be disrupted in migraine (83–88). In adult patients, reduced cortical thickness of the precuneus has been reported together with abnormalities in other DMN regions such as the medial prefrontal cortex and hippocampus (62).

Interestingly, MSN alterations in the precuneus were particularly evident in male patients with nausea and vomiting. As the precuneus contributes to the integration of visceral sensory inputs with conscious awareness (46), these findings may indicate sex-specific vulnerability in processing internal bodily states. Disrupted MSN architecture in the precuneus could therefore provide a neural correlate for the variability of autonomic symptoms across sex. The sex-related MSN

differences observed in our sample are consistent with previous morphometric studies conducted in children and adult migraine (6,49,81) and reinforce the view that sex modulates almost all of the major pathways impaired in migraine.

Limitations

The main limitation of the present study is its retrospective design, although this was partially mitigated by the application of strict inclusion and exclusion criteria for both patients and controls. Another limitation concerns the relatively small sample size, which, although comparable to previous pediatric neuroimaging studies, may have reduced the power to detect more subtle effects. Finally, clinical data were collected at a single time point, preventing us from assessing the longitudinal stability of MSN alterations. Future prospective and multicenter studies with larger cohorts are warranted to confirm and extend our findings.

Conclusions

MSM revealed significant alterations of morphometric similarity networks in children and adolescents with migraine without aura. Sex emerged as the main modulatory factor, differentiating male and female patients through distinct patterns of cortical network engagement across frontal, temporal, cingulate and parietal regions.

These findings suggest that male and female brains may process migraine through partially distinct neural "orchestras," each emphasizing different network sections (sensory–affective in males and cognitive–attentive in females) to produce a shared clinical experience.

The identification of in-vivo biomarkers of cortical and connectivity anomalies, together with demographic and clinical stratification, represents a step toward precision medicine in migraine and may inform more tailored therapeutic strategies for young patients.

Article highlights

- MSM revealed significant cortical network alterations in children and adolescents with migraine without aura.
- Sex emerged as the strongest modulatory factor, distinguishing male and female patients through distinct patterns of network involvement.
- Temporal, cingulate, frontal and parietal regions showed the most consistent alterations, involving the executive, nociceptive and default mode networks.
- Findings highlight sex-dependent neural "orchestras" underlying a shared clinical phenotype, supporting precision approaches to children and adolescents with migraine.

ORCID iDs

Laura Papetti https://orcid.org/0000-0002-3336-9205
Antonio Napolitano https://orcid.org/0000-0003-3258-6846
Greta Pirani https://orcid.org/0000-0001-8646-8752
Gabriele Monte https://orcid.org/0000-0002-4763-7784
Massimiliano Valeriani https://orcid.org/0000-0001-6602-103X

Ethical considerations

The study was conducted in accordance with the Declaration of Helsinki and approved by the Institutional Research Committee.

Consent to participate

Written informed consent was obtained from all patients or their parents before MRI examination.

Consent for publishing

All authors have read and approved the final version of the manuscript submitted for publication.

Author contributions

LP was responsible for conceptualization and writing the final accepted version of the manuscript. AG was responsible for conceptualization and writing the first draft. AN was responsible for data analysis and interpretation of results. GP and GB were responsible for statistical analysis. GM, GS and were responsible for patients and controls selection. FD, MCRE, MV, AC and GM were responsible for methodology and data acquisition. CG was responsible for manuscript revision. DL and MV were responsible for study supervision and critical revision of the manuscript.

Funding

The authors disclosed receipt of the following financial support for the research, authorship, and/or publication of this article: This work was supported by the Italian Ministry of Health (Current Research funds) and by the IHS Research into Headache in Children and Adolescents Seed Grant, Ministero della Salute (grant number Current Research).

Declaration of conflicting interests

The authors declared no potential conflicts of interest with respect to the research, authorship and/or publication of this article.

Data availability

Data are available from the corresponding author, upon reasonable request.

Supplemental material

Supplemental material for this article is available online.

References

1. Zhang J, Wu YL, Su J, et al. Assessment of gray and white matter structural alterations in migraineurs without aura. *J Headache Pain* 2017; 18: 74.
2. Liu J, Zhao L, Li G, et al. Hierarchical alteration of brain structural and functional networks in female migraine sufferers. *PLoS One* 2012; 7: e51250.
3. Jin C, Yuan K, Zhao L, et al. Structural and functional abnormalities in migraine patients without aura. *NMR Biomed* 2013; 26: 58–64.
4. Chong CD, Schwedt TJ and Dodick DW. Migraine: what imaging reveals. *Curr Neurol Neurosci Rep* 2016; 16: 64.
5. Schwedt TJ, Chong CD, Peplinski J, et al. Persistent post-traumatic headache vs. migraine: an MRI study demonstrating differences in brain structure. *J Headache Pain* 2017; 18: 87.
6. Faria V, Erpelding N, Lebel A, et al. The migraine brain in transition: girls vs boys. *Pain* 2015; 156: 2212–2221.
7. Hubbard CS, Becerra L, Smith JH, et al. Brain changes in responders vs. *Non-Responders in Chronic Migraine: Markers of Disease Reversal. Front Hum Neurosci* 2016; 10: 97.
8. Burke MJ, Joutsa J, Cohen AL, et al. Mapping migraine to a common brain network. *Brain* 2020; 143: 541–553.
9. Silvestro M, Tessitore A, Caiazzo G, et al. Disconnectome of the migraine brain: a "connectopathy" model. *J Headache Pain* 2021; 22: 102.
10. Messina R, Rocca MA, Colombo B, et al. Cortical abnormalities in patients with migraine: a surface-based analysis. *Radiology* 2013; 268: 170–180.
11. Masson R, Demarquay G, Meunier D, et al. Is migraine associated to brain anatomical alterations? New data and coordinate-based meta-analysis. *Brain Topogr* 2021; 34: 384–401.
12. Wang HZ, Wang WH, Shi HC, et al. Is there a reliable brain morphological signature for migraine? *J Headache Pain* 2020; 21: 89.
13. Seidlitz J, Váša F, Shinn M, et al. Morphometric similarity networks detect microscale cortical organization and predict inter-individual cognitive variation. *Neuron* 2018; 97: 231–247.e7.
14. Morgan SE, Seidlitz J, Whitaker KJ, et al. Cortical patterning of abnormal morphometric similarity in psychosis is associated with brain expression of schizophrenia-related genes. *Proc Natl Acad Sci U S A* 2019; 116: 9604–9609.
15. Wang Y, Dong D, Chen X, et al. Individualized morphometric similarity predicts body mass index and food approach behavior in school-age children. *Cereb Cortex* 2023; 33: 4794–4805.
16. King DJ and Wood AG. Clinically feasible brain morphometric similarity network construction approaches with restricted magnetic resonance imaging acquisitions. *Netw Neurosci* 2020; 4: 274–291.
17. Zhang Y, Ma M, Xie Z, et al. Bridging the gap between morphometric similarity mapping and gene transcription in Alzheimer's disease. *Front Neurosci* 2021; 15: 731292.
18. Li X, Hao H, Li Y, et al. Menstrually-related migraine shapes the structural similarity network integration of brain. *Cereb Cortex* 2023; 33: 9867–9876.
19. Christensen RH, Al-Khazali HM, Ashina M, et al. Differences in cortical morphometry between persistent post-traumatic headache, migraine and control controls. *Cephalalgia* 2025; 45: 3331024251362830.
20. Headache classification committee of the international headache society (IHS) the international classification of headache disorders, 3rd edition. *Cephalalgia* 2018; 38: 1–211.
21. Kacperski J and Hershey AD. Preventive drugs in childhood and adolescent migraine. *Curr Pain Headache Rep* 2014; 18: 422.
22. Cammarota F, De Icco R, Vaghi G, et al. High-frequency episodic migraine: time for its recognition as a migraine subtype? *Cephalalgia* 2024; 44: 3331024241291578.
23. Guarnera A, Bottino F, Napolitano A, et al. Early alterations of cortical thickness and gyrification in migraine without aura: a retrospective MRI study in pediatric patients. *J Headache Pain* 2021; 22: 79.
24. Rosen AFG, Roalf DR, Ruparel K, et al. Quantitative assessment of structural image quality. *Neuroimage* 2018; 169: 407–418.
25. Dale AM, Fischl B and Sereno MI. Cortical surface-based analysis. I. Segmentation and surface reconstruction. *Neuroimage* 1999; 9: 179–194.
26. Fischl B and Dale AM. Measuring the thickness of the human cerebral cortex from magnetic resonance images. *Proc Natl Acad Sci U S A* 2000; 97: 11050–11055.
27. Panizzon MS, Fennema-Notestine C, Eyler LT, et al. Distinct genetic influences on cortical surface area and cortical thickness. *Cereb Cortex* 2009; 19: 2728–2735.
28. RaviPrakash H, Anwar SM, Biassou NM, et al. Morphometric and functional brain connectivity differentiates chess masters from amateur players. *Front Neurosci* 2021; 15: 629478.
29. Schaer M, Cuadra MB, Tamarit L, et al. A surface-based approach to quantify local cortical gyrification. *IEEE Trans Med Imaging* 2008; 27: 161–170.
30. Li S, Yuan X, Pu F, et al. Abnormal changes of multidimensional surface features using multivariate pattern classification in amnestic mild cognitive impairment patients. *J Neurosci* 2014; 34: 10541–10553.
31. Pienaar R, Fischl B, Caviness V, et al. A methodology for analyzing curvature in the developing brain from preterm to adult. *Int J Imaging Syst Technol* 2008; 18: 42–68.
32. Lyu I, Kim SH, Girault JB, et al. A cortical shape-adaptive approach to local gyrification index. *Med Image Anal* 2018; 48: 244–258.
33. Alexander-Bloch A, Raznahan A, Bullmore E, et al. The convergence of maturational change and structural covariance in human cortical networks. *J Neurosci* 2013; 33: 2889–2899.
34. Desikan RS, Ségonne F, Fischl B, et al. An automated labeling system for subdividing the human cerebral cortex on MRI scans into gyral based regions of interest. *Neuroimage* 2006; 31: 968–980.
35. Yang S, Wagstyl K, Meng Y, et al. Cortical patterning of morphometric similarity gradient reveals diverged hierarchical organization in sensory-motor cortices. *Cell Rep* 2021; 36: 109582.
36. Maleki N, Linnman C, Brawn J, et al. Her versus his migraine: multiple sex differences in brain function and structure. *Brain* 2012; 135: 2546–2559.

37. Buse DC, Loder EW, Gorman JA, et al. Sex differences in the prevalence, symptoms, and associated features of migraine, probable migraine and other severe headache: results of the American migraine prevalence and prevention (AMPP) study. *Headache* 2013; 53: 1278–1299.
38. Casucci G, Villani V, d'Onofrio F, et al. Migraine and lifestyle in childhood. *Neurol Sci* 2015; 36: 97–100.
39. Martin VT, Lee J and Behbehani MM. Sensitization of the trigeminal sensory system during different stages of the rat estrous cycle: implications for menstrual migraine. *Headache* 2007; 47: 552–563.
40. Bigal ME, Ashina S, Burstein R, et al. Prevalence and characteristics of allodynia in headache sufferers: a population study. *Neurology* 2008; 70: 1525–1533.
41. Ferrari A, Tiraferri I, Neri L, et al. Why pharmacokinetic differences among oral triptans have little clinical importance: a comment. *J Headache Pain* 2011; 12: 5–12.
42. Webb ME, Amoozegar F and Harris AD. Magnetic resonance imaging in pediatric migraine. *Can J Neurol Sci* 2019; 46: 653–665.
43. Apkarian AV, Bushnell MC, Treede RD, et al. Human brain mechanisms of pain perception and regulation in health and disease. *Eur J Pain* 2005; 9: 463–484.
44. Seminowicz DA and Moayedi M. The dorsolateral prefrontal Cortex in acute and chronic pain. *J Pain* 2017;18: 1027–1035.
45. Schwedt TJ, Chiang CC, Chong CD, et al. Functional MRI of migraine. *Lancet Neurol* 2015; 14: 81–91.
46. Cavanna AE and Trimble MR. The precuneus: a review of its functional anatomy and behavioural correlates. *Brain* 2006; 129: 564–583.
47. Menon V. Large-scale brain networks and psychopathology: a unifying triple network model. *Trends Cogn Sci* 2011; 15: 483–506.
48. Borsook D, Veggeberg R, Erpelding N, et al. The Insula: a "hub of activity" in migraine. *Neuroscientist* 2016; 22: 632–652.
49. Shallice T and Burgess PW. Deficits in strategy application following frontal lobe damage in man. *Brain* 1991; 114: 727–741.
50. Robbins TW. Shifting and stopping: fronto-striatal substrates, neurochemical modulation and clinical implications. *Philos Trans R Soc Lond B Biol Sci* 2007; 362: 917–932.
51. Schmitz N, Arkink EB, Mulder M, et al. Frontal lobe structure and executive function in migraine patients. *Neurosci Lett* 2008; 440: 92–96.
52. Kim JH, Suh SI, Seol HY, et al. Regional grey matter changes in patients with migraine: a voxel-based morphometry study. *Cephalalgia* 2008; 28: 598–604.
53. Peyron R, García-Larrea L, Grégoire MC, et al. Haemodynamic brain responses to acute pain in humans: sensory and attentional networks. *Brain* 1999; 122: 1765–1780.
54. Peyron R, Laurent B and García-Larrea L. Functional imaging of brain responses to pain. A review and meta-analysis (2000). *Neurophysiol Clin* 2000; 30: 263–288.
55. Oshiro Y, Quevedo AS, McHaffie JG, et al. Brain mechanisms supporting spatial discrimination of pain. *J Neurosci* 2007; 27: 3388–3394.
56. Price DD. Central neural mechanisms that interrelate sensory and affective dimensions of pain. *Mol Interv* 2002; 2: 392–403.
57. Chiapparini L, Ferraro S, Grazzi L, et al. Neuroimaging in chronic migraine. *Neurol Sci* 2010; 31: S19–S22.
58. Dai Z, Zhong J, Xiao P, et al. Gray matter correlates of migraine and sex effect: a meta-analysis of voxel-based morphometry studies. *Neuroscience* 2015; 299: 88–96.
59. Hougaard A, Amin FM, Magon S, et al. No abnormalities of intrinsic brain connectivity in the interictal phase of migraine with aura. *Eur J Neurol* 2015; 22: 702-e46.
60. Rocca MA, Messina R, Colombo B, et al. Structural brain MRI abnormalities in pediatric patients with migraine. *J Neurol* 2014; 261: 350–357.
61. Rocca MA, Ceccarelli A, Falini A, et al. Diffusion tensor magnetic resonance imaging at 3.0 tesla shows subtle cerebral grey matter abnormalities in patients with migraine. *J Neurol Neurosurg Psychiatry* 2006; 77: 686–689.
62. Celle S, Créac'h C, Boutet C, et al. Elderly patients with ongoing migraine show reduced gray matter volume in second somatosensory Cortex. *J Oral Facial Pain Headache* 2018; 32: 67–74.
63. Özge A, Abu-Arafeh I, Gelfand AA, et al. Experts' opinion about the pediatric secondary headaches diagnostic criteria of the ICHD-3 beta. *J Headache Pain* 2017; 18: 113.
64. De Pauw R, Coppieters I, Caeyenberghs K, et al. Associations between brain morphology and motor performance in chronic neck pain: a whole-brain surface-based morphometry approach. *Hum Brain Mapp* 2019; 40: 4266–4278.
65. Budell L, Kunz M, Jackson PL, et al. Mirroring pain in the brain: emotional expression versus motor imitation. *PLoS One* 2015; 10: e0107526.
66. Rocca MA, Ceccarelli A, Falini A, et al. Brain gray matter changes in migraine patients with T2-visible lesions: a 3-T MRI study. *Stroke* 2006; 37: 1765–1770.
67. Godinho F, Magnin M, Frot M, et al. Emotional modulation of pain: is it the sensation or what we recall? *J Neurosci* 2006; 26: 11454–11461.
68. Palermo S, Benedetti F, Costa T, et al. Pain anticipation: an activation likelihood estimation meta-analysis of brain imaging studies. *Hum Brain Mapp* 2015; 36: 1648–1661.
69. Mainero C, Boshyan J and Hadjikhani N. Altered functional magnetic resonance imaging resting-state connectivity in periaqueductal gray networks in migraine. *Ann Neurol* 2011; 70: 838–845.
70. Craig AD. How do you feel — now? The anterior insula and human awareness. *Nat Rev Neurosci* 2009; 10: 59–70. Nat Rev Neurosci. 2009.
71. Noseda R and Burstein R. Migraine pathophysiology: anatomy of the trigeminovascular pathway and associated neurological symptoms, CSD, sensitization and modulation of pain. *Pain* 2013; 154:S44–S53.
72. Liu J, Lan L, Li G, et al. Migraine-related gray matter and white matter changes at a 1-year follow-up evaluation. *J Pain* 2013; 14: 1703–1708.
73. Valfrè W, Rainero I, Bergui M, et al. Voxel-based morphometry reveals gray matter abnormalities in migraine. *Headache* 2008; 48: 109–117.

74. Kozlovskiy SA, Vartanov AV, Pyasik MM, et al. The cingulate cortex and human memory process. *Psychol Russ State Art* 2012; 5: 231.
75. Hadland KA, Rushworth MFS, Gaffan D, et al. The effect of cingulate lesions on social behaviour and emotion. *Neuropsychologia* 2003; 41: 919–931.
76. Kozlovskiy S, Vartanov A, Pyasik M, et al. Anatomical characteristics of cingulate cortex and neuropsychological memory tests performance. *Procedia Soc Behav Sci* 2013; 86: 128–133.
77. Hayden BY and Platt ML. Neurons in anterior cingulate cortex multiplex information about reward and action. *J Neurosci* 2010; 30: 3339–3346.
78. Adams R and David AS. Patterns of anterior cingulate activation in schizophrenia: a selective review. *Neuropsychiatr Dis Treat* 2007; 3: 87–101.
79. Drevets WC, Savitz J and Trimble M. The subgenual anterior cingulate cortex in mood disorders. *CNS Spectr* 2008; 13: 663–681.
80. Maleki N, Becerra L, Brawn J, et al. Concurrent functional and structural cortical alterations in migraine. *Cephalalgia* 2012; 32: 607–620.
81. Eck J, Richter M, Straube T, et al. Affective brain regions are activated during the processing of pain-related words in migraine patients. *Pain* 2011; 152: 1104–1113.
82. Crockford DN, Goodyear B, Edwards J, et al. Cue-induced brain activity in pathological gamblers. *Biol Psychiatry* 2005; 58: 787–795.
83. Haldane M, Cunningham G, Androutsos C, et al. Structural brain correlates of response inhibition in Bipolar Disorder I. *J Psychopharmacol* 2008; 22: 138–143.
84. de Tommaso M, Ambrosini A, Brighina F, et al. Altered processing of sensory stimuli in patients with migraine. *Nat Rev Neurol* 2014; 10: 144–155.
85. Magon S, May A, Stankewitz A, et al. Cortical abnormalities in episodic migraine: a multi-center 3T MRI study. *Cephalalgia* 2019; 39: 665–673.
86. Harriott AM and Schwedt TJ. Migraine is associated with altered processing of sensory stimuli. *Curr Pain Headache Rep* 2014; 18: 458.
87. Buckner RL, Andrews-Hanna JR and Schacter DL. The brain's default network: anatomy, function, and relevance to disease. *Ann N Y Acad Sci* 2008; 1124: 1–38.
88. Simpson JR Jr, Snyder AZ, Gusnard DA, et al. Emotion-induced changes in human medial prefrontal cortex: i. During cognitive task performance. *Proc Natl Acad Sci U S A* 2001; 98: 683–687.